CHAPTER IV
RESULTS AND DISCUSSION

4.1 Characterization of TUD-1 and Pd-TUD-1

4.1.1 X-Ray Diffraction (XRD) of TUD-1 and Pd-TUD-1

Structures of TUD-1and Pd-TUD-1 synthesized by sol-gel and impregnation techniques, respectively, were characterized using XRD. Typically, the XRD pattern of TUD-1 is a single broad peak at low 2θ angle between 0.2° and 10°, with a maximum peak around 1°, indicative of mesoporous structure, as also observed in our cases of both TUD-1 and Pd-TUD-1 with various percentages of Pd (Fig. 4.1). Moreover, higher order Bragg reflections were not observed for all samples, indicating the disordered mesostructured materials (Tanglumlert *et al.*, 2011), and also confirming the presence of amorphous structure of TUD-1 (Angevine *et al.*, 2008).The intensity of the reflection decreased with increasing Pd content, implying that the short-range order was increasingly disrupted by Pd, resulting in the initial structures to be shortened and more heterogeneous, as discussed by Saad, *et al.* in 2005. They explained the influence of metal oxide particles, i.e. PdO in this case (Fig. 4.2), on the integrity of the mesoporous structure where the particles dispersed into the interconnecting pores and on the surface.

To verify the presence of Pd and characterize the type of Pd species loaded on TUD-1 support, wide angle XRD was also carried out at an angle range of 20–60 degree of 2θ. As shown in Fig. 4.2, the very broad band at about 23° was attributed to amorphous silica matrix of TUD-1 and the intense peaks at around 34°, 42°, and 55° correspond to PdO {101}, PdO {110}, and PdO {112}, respectively (Abate *et al.*, 2011). The peak intensity obviously increases with the increase of Pd content. Unfortunately, Pd° was not able to observe in our case.

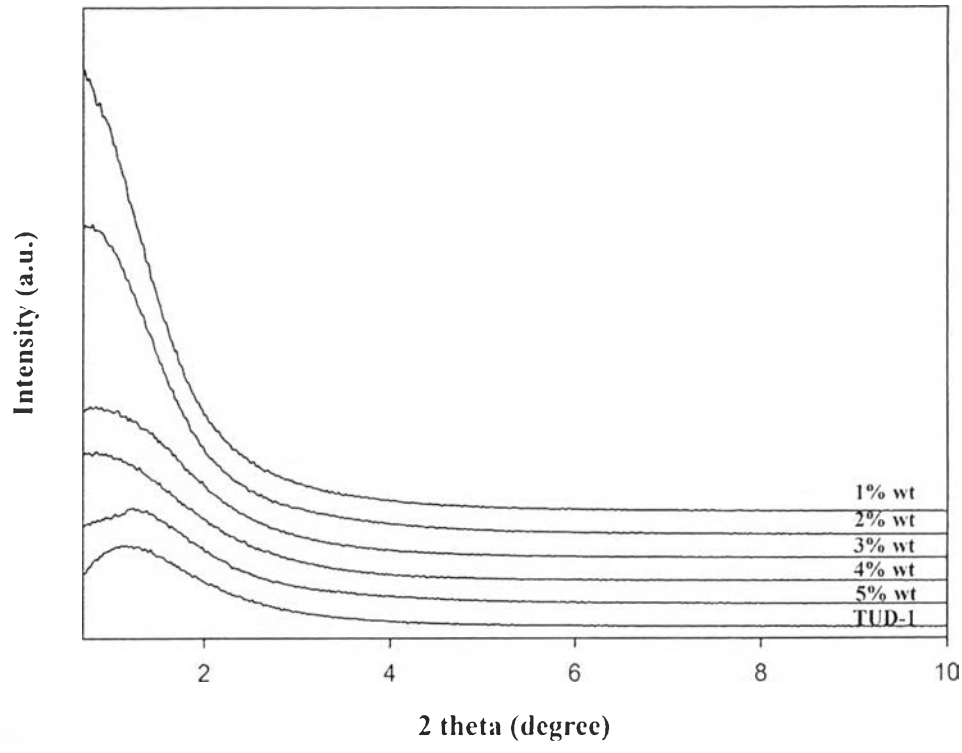

Figure 4.1 XRD patterns of TUD-1 and Pd-TUD-1 synthesized with various amounts of Pd.

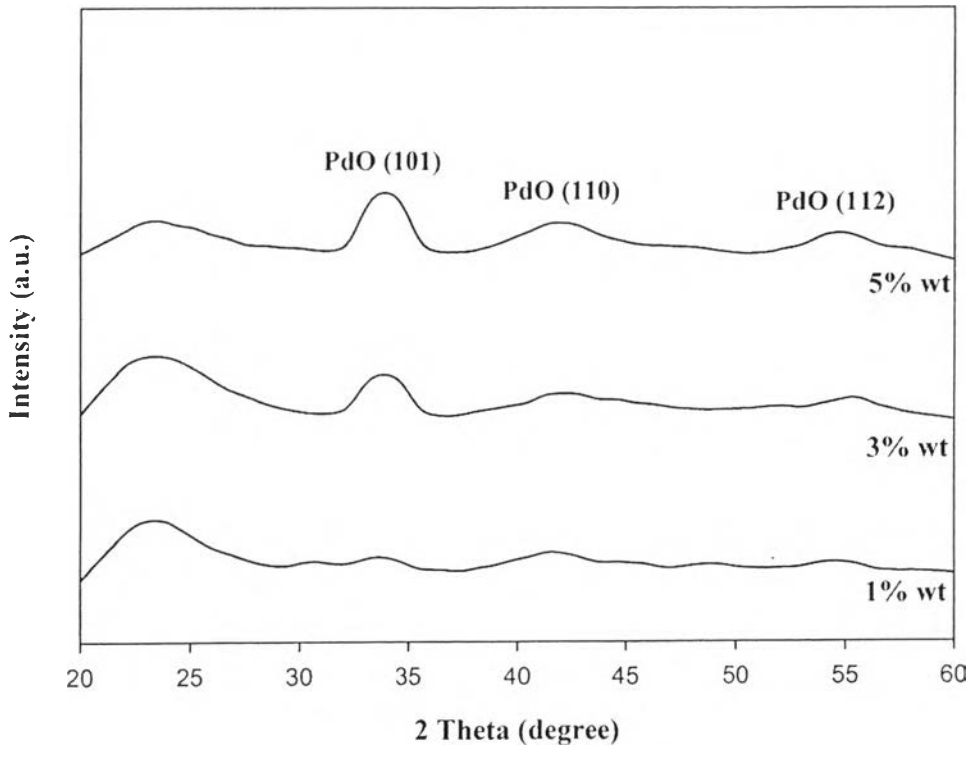

Figure 4.2 Wide angle XRD patterns of Pd-TUD-1 with various Pd amounts

4.1.2 Scanning Electron Microscopy (SEM) and Transmission Electron Microscopy (TEM) of TUD-1 and Pd-TUD-1

SEM images in Fig. 4.3 of pure TUD-1 synthesized by sol-gel technique show irregularly-shaped particles without well-defined morphology. The particles of TUD-1 had the average diameter of 500 nm and were well sorted. Such morphology is similar to the results described by Arafat *et al.* (2009).

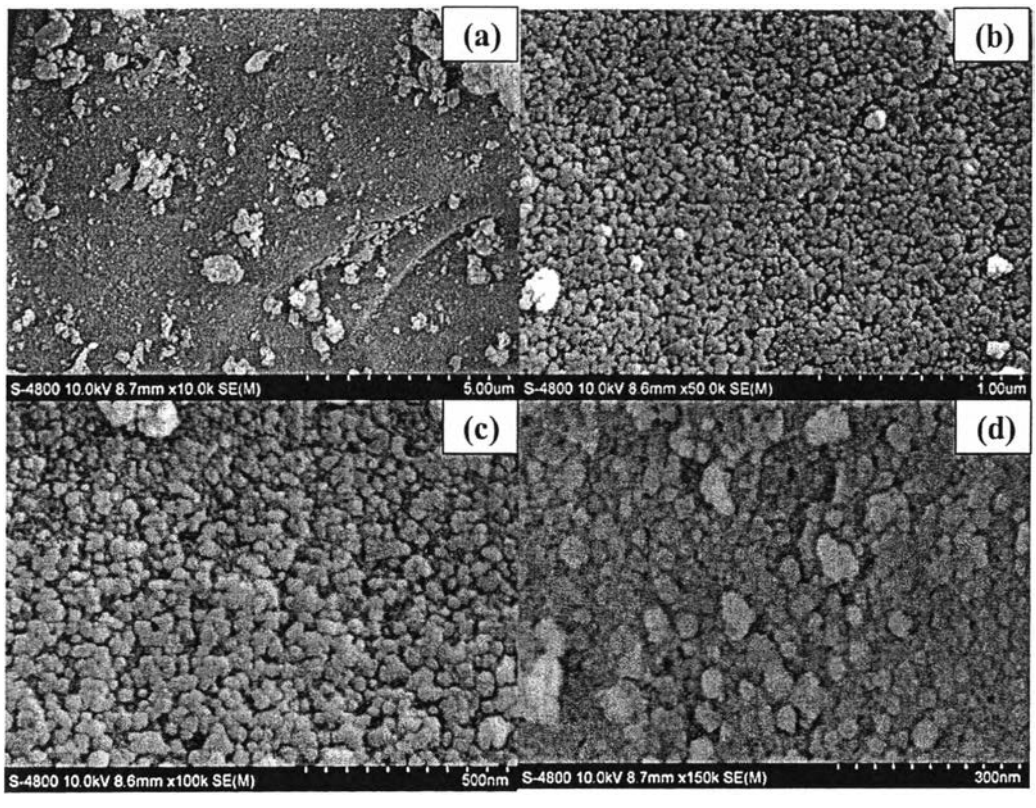

Figure 4.3 SEM images of TUD-1synthesized by sol-gel technique, taken at magnifications of (a) 10k, (b) 50k, (c) 100k, and (d) 150k.

SEM images of Pd-TUD-1 (Fig. 4.4) were similar to that of the unloaded TUD-1. This might confirm that loading Pd onto TUD-1 still maintained the shape of the support.

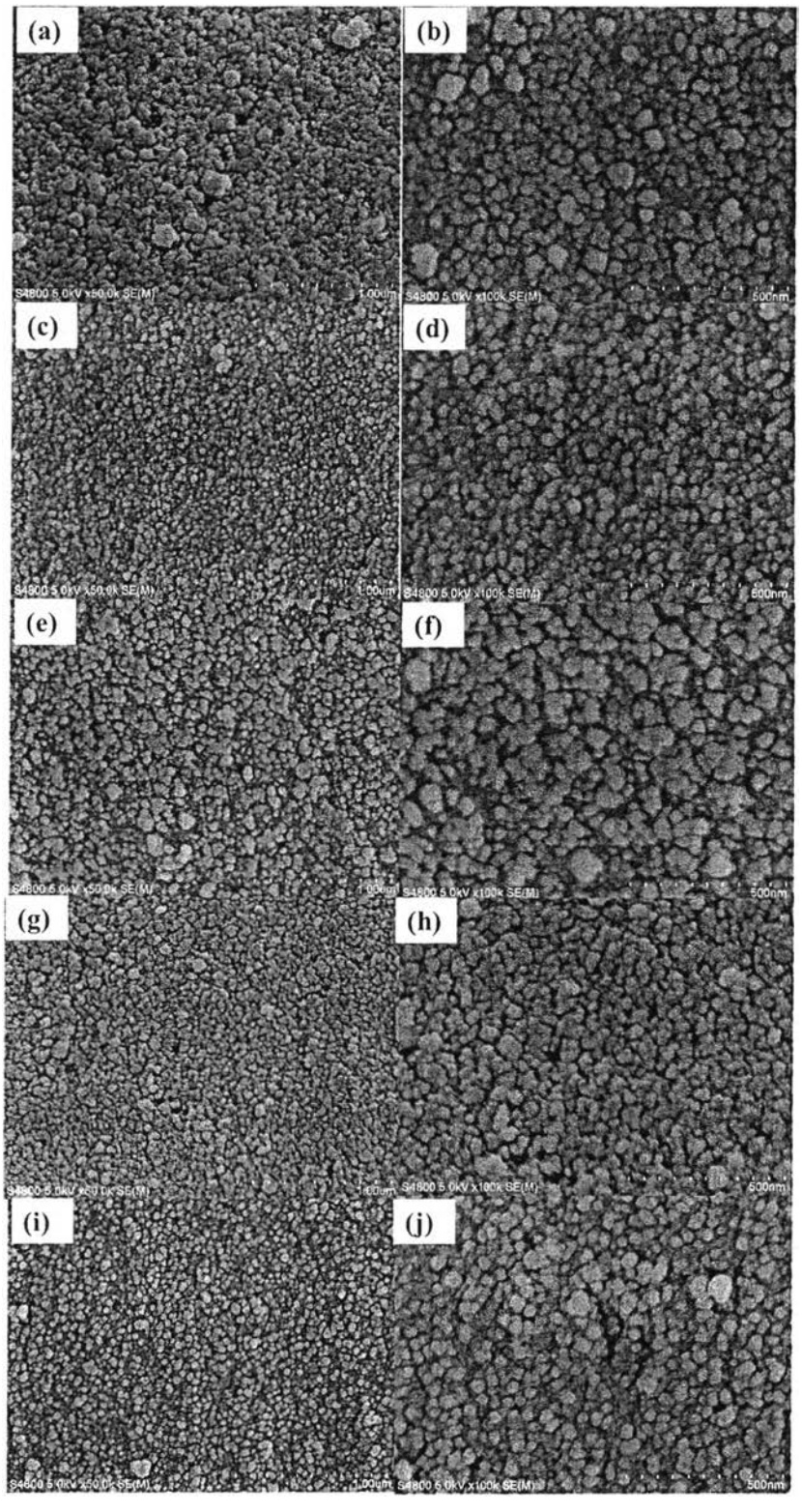

Figure 4.4 SEM images of Pd-TUD-1 synthesized by impregnation technique with different Pd contents: (a,b) 1, (c, d) 2, (e, f) 3, (g, h) 4, and (i, j) 5%Pd-TUD-1 (a, c, e, and g taken at magnification of 50k whereas b, d, f, and h of 100k).

To confirm further, TEM analysis was also conducted to determine the physical structure of different Pd loadings onto TUD-1, as can be seen in Fig. 4.5. The images clearly illustrate the sponge-like structure, three-dimensionally connected mesoporous network of Pd-TUD-1 prepared by impregnation technique, consistent with the work reported by Wang *et al.* in2011. The images also show small and large pores well dispersed throughout the entire surface and Pd species in 5% Pd-TUD-1 were clearly seen as agglomeration encapsulated by amorphous silica. However, Pd species could not be observed for 1% Pd-TUD-1, consistent with Srinivasu *et al.* (2010) who also observed that as increasing the Pd loading, agglomeration tended to occur.

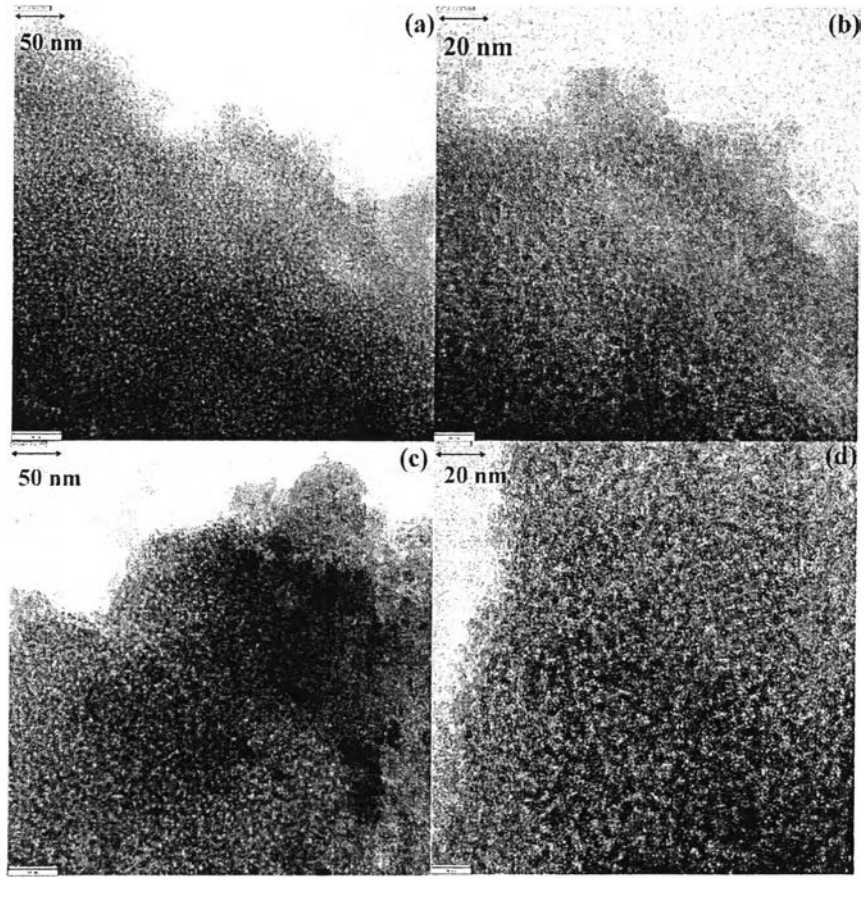

Figure 4.5 TEM images of (a, b) 1 and (c, d) 5% Pd-TUD-1 synthesized by impregnation technique (a and c taken at the magnification of 50k, b and d at the magnification of 100k).

4.1.3 Brunauer Emmett Teller (BET) of TUD-1 and Pd-TUD-1

BET surface area, pore volume, and pore size of our synthesized samples, i.e., TUD-1 and Pd-TUD-1, were analyzed using nitrogen adsorption/ desorption isotherms. A summary of the results is given in Table 4.1. The N_2 adsorption–desorption isotherms of the unloaded TUD-1 are illustrated in Fig. 4.6. Due to capillary condensation in the mesopores, according to IUPAC classification, Fig. 4.6(a) shows type IV isotherms of TUD-1 with an H2-type hysteresis loop, corresponding to mesopores materials at the relative pressures starting from 0.4 to 0.7 (Tanglumlert *et al.*, 2011). In addition, the pore-size distribution of TUD-1 is quite narrow at around 4 nm (Fig. 4.6(b)).

Table 4.1 Specific surface area, pore volume, and pore diameter of unloaded TUD-1 and various percent weight of Pd loaded on TUD-1 via impregnation technique

Sample	Surface area (m^2/g)	Pore volume (ml/g)	Pore diameter (nm)
	Synthesis via sol-gel technique		
TUD-1	808.0	0.765	3.78
	Synthesis via impregnation technique		
1%wt Pd-TUD-1	552.0	0.671	4.86
2%wt Pd-TUD-1	534.6	0.612	4.58
3%wt Pd-TUD-1	493.4	0.567	4.60
4%wt Pd-TUD-1	475.8	0.547	4.60
5%wt Pd-TUD-1	534.4	0.601	4.50

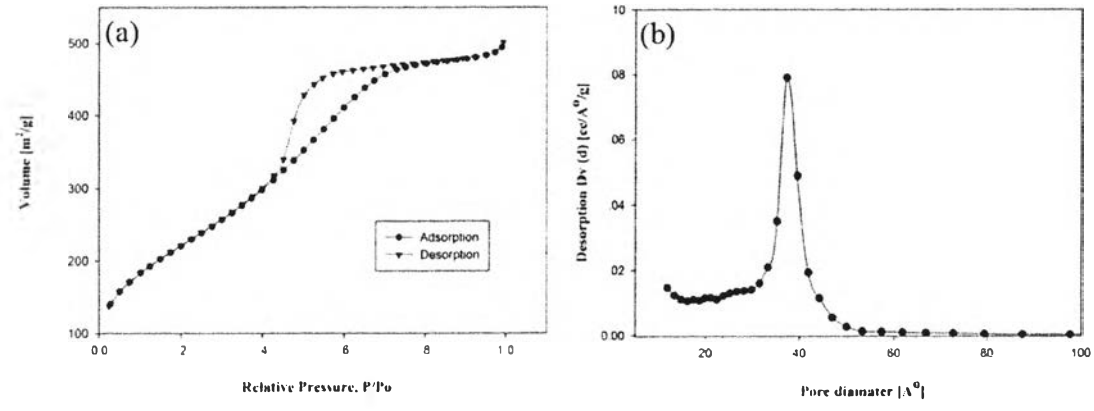

Figure 4.6 (a) The isotherms and (b) the narrow pore size distribution of TUD-1.

The BET results of Pd-TUD-1 with different Pd contents derived from impregnation techniques are plotted in Fig. 4.7. All results show type IV isotherms with an H2-type hysteresis loop at relative pressures from 0.4 to 0.7 and narrow pore size distributions of Pd-TUD-1 at around 4 nm (inset). From Table 4.1, the surface area was found to be largely affected by the Pd loading. When more contents of Pd species were loaded onto TUD-1, the surface areas of Pd-TUD-1 were found to decrease due to the blockage of PdO in the pores of TUD-1 during the impregnation process, causing the distortion of the TUD-1 structure by PdO (Han *et al.*, 2007). However, the specific surface area of 5% Pd-TUD-1 was higher than 3% and 4% Pd-TUD-1. This may resulted from larger agglomerated Pd species, not able to fill in the structural pores of TUD-1, as a result, giving no pore distortion and consequently, providing higher surface area. Thus, the remnant Pd particles were probably distributed on the surface of the TUD-1 support (Li *et al.*, 2011). This hypothesis can be supported by SEM and TEM images of 5%Pd-TUD-1 (Fig. 4.4 and 4.5), showing agglomerated Pd with dark color.

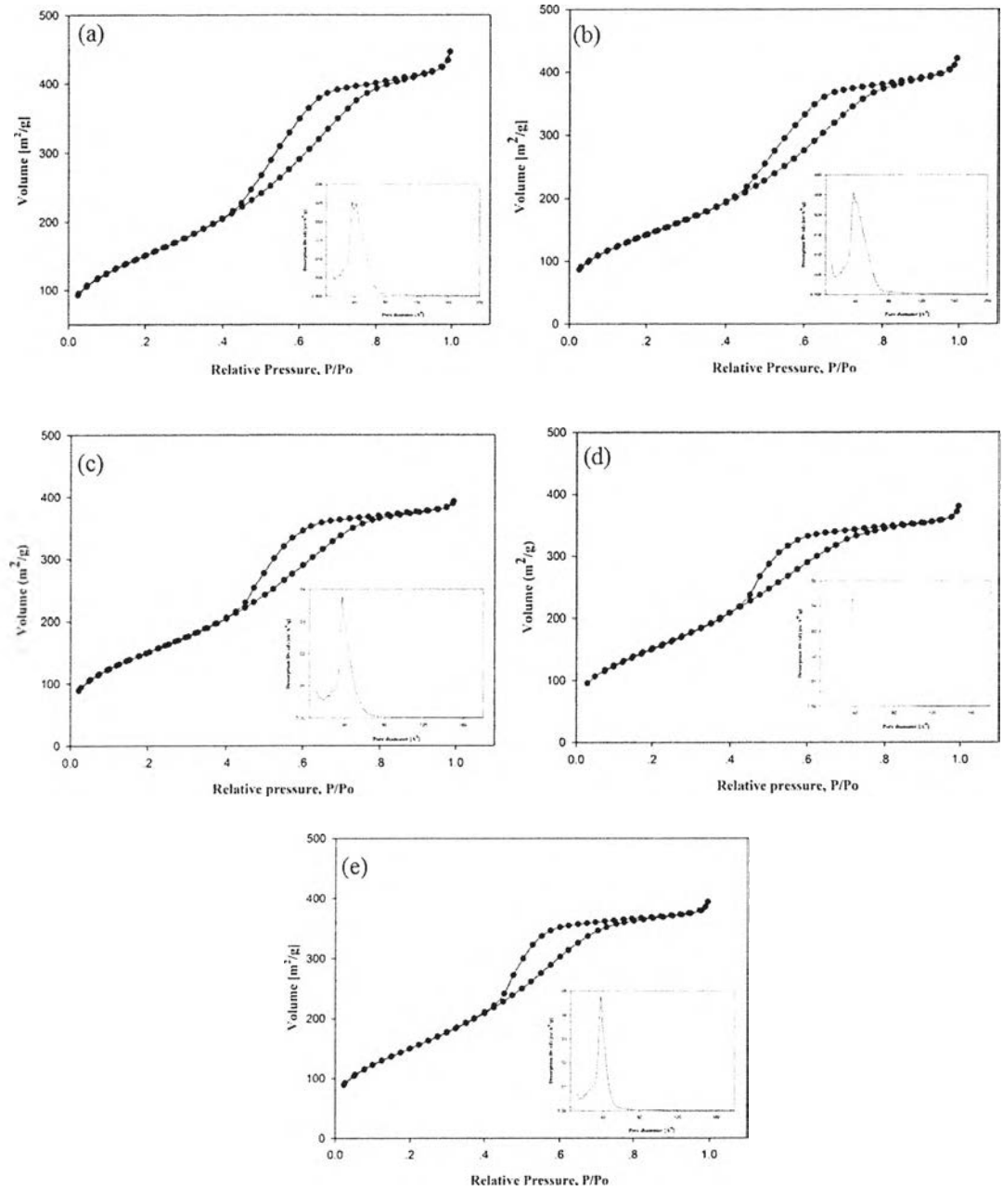

Figure 4.7 The isotherms and the narrow pore size distribution (inset) of Pd-TUD-1 with various Pd amounts of (a) 1, (b) 2, (c) 3, (d) 4, and (e) 5% Pd-TUD-1 synthesized via impregnation technique.

4.1.4 X-Ray Fluorescence Spectrophotometer (XRF)

Chemical compositions of the samples were analyzed using XRF, as summarized in Table 4.2, providing the percentages of Si, O, and Pd elements in TUD-1 and Pd-TUD-1.As can be seen, the percentage of Pd was found to be much less than the added amount. One possible reason might be that, the impregnation always causes agglomeration of the loading species, resulting in non-homogeneity of the catalyst. Moreover, the amount of the Pd loading onto TUD-1 support was very small (ca.0.003–0.016 g of Pd), the sample analyzed thus mainly contained silica.

Table 4.2 XRF analysis of Pd-TUD-1 synthesized using various Pd amounts

Materials	Si (%)	O (%)	Pd (%)
TUD-1	31.40	68.60	-
1% Pd-TUD-1	36.13	63.86	0.01
2% Pd-TUD-1	36.83	63.15	0.02
3% Pd-TUD-1	39.93	60.03	0.04
4% Pd-TUD-1	37.91	62.04	0.05
5% Pd-TUD-1	41.41	58.53	0.06

4.1.5 Diffuse reflectance Ultraviolet-Visible Spectrometer (DR-UV)

To confirm whether Pd species were in framework, DR-UV was conducted, as shown in Fig. 4.8, showing the DRUV spectra of TUD-1 and Pd-TUD-1 with various Pd contents. It can be noticed that all Pd-TUD-1 samples shows characteristic absorption band around 320–370 nm and 440-500 nm, resulting from the charge transfer band and d-d transitions band of Pd^{2+}, respectively (Pestryakov *et al.*, 2003). The wavenumber at 440–500 nm of the d-d transition band can attribute to the presence of PdO over the TUD-1 structural surface (López-Gaona *et al.*, 2010). These results can also confirm the XRD result given in Fig. 4.2 that Pd° was not formed in our Pd-TUD-1 products. Therefore, we can conclude that Pd was in the

form of only PdO species during Pd-TUD-1 formation and dispersed as an extra framework.

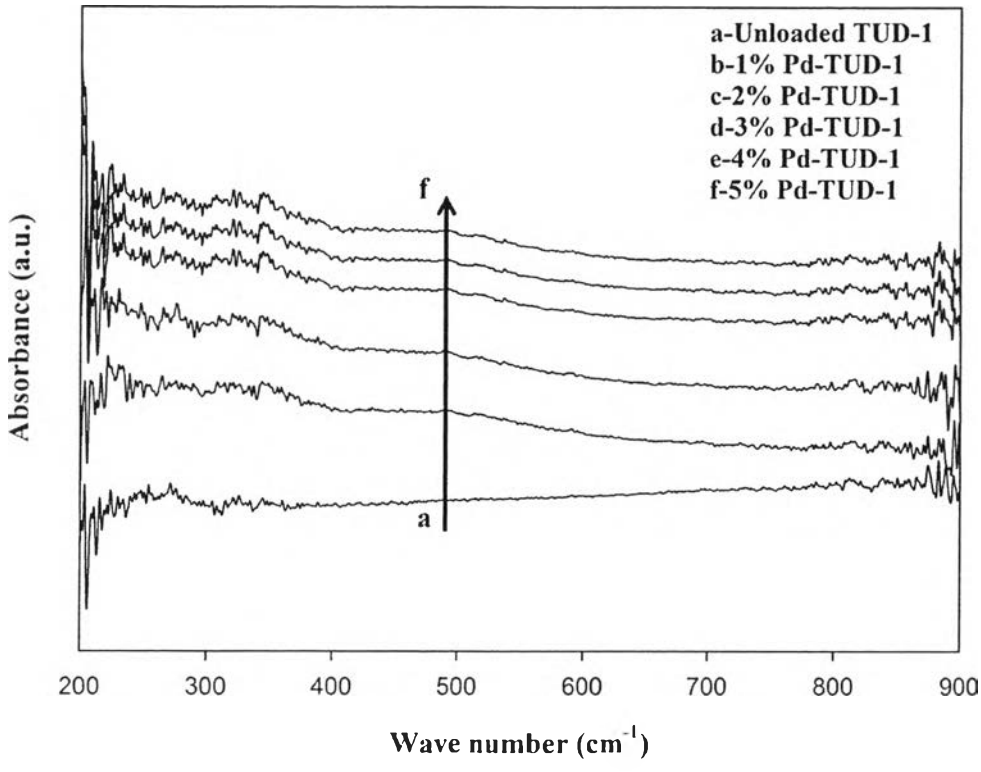

Figure 4.8 UV-visible absorption spectra of TUD-1 and Pd-TUD-1synthesized with various Pd amounts

4.1.6 Temperature-Programmed Reduction (TPR)

This method was used to examine the reducibility of palladium species in Pd-TUD-1. Figure 4.9 shows the TPR results of TUD-1 impregnated with the Pd content of 1, 3, and 5%. Panpranot *et al.* (2004) reported that Pd on catalytic support prepared from using palladium nitrate was in the form of PdO species agglomerated on the support surface. If PdO species interact weakly with the supports, the PdO species can be reduced readily to be H_xPd (Palladium hydride) at an ambient temperature when hydrogen is introduced into the system (not shown in Fig. 4.9), as demonstrated by Panpranot *et al.*(2004). The palladium hydride would generate H_2 when raising the temperature to around 100 °C, as an inverse peak, as described by Lopez-Gaona *et al.* (2010). Thus, the more PdO species as for 5%wt Pd-TUD-1, the more H_2 generated. They also suggested that such an inverse peak

effect might be indicative of large Pd particles on the supports. The peak became more negative when Pd concentration on the supports increased, resulting in the higher release of chemisorbed hydrogen. In addition, the amount of H_2 released from Pd could decrease when the metal dispersion increased (López-Gaona *et al.*, 2010).

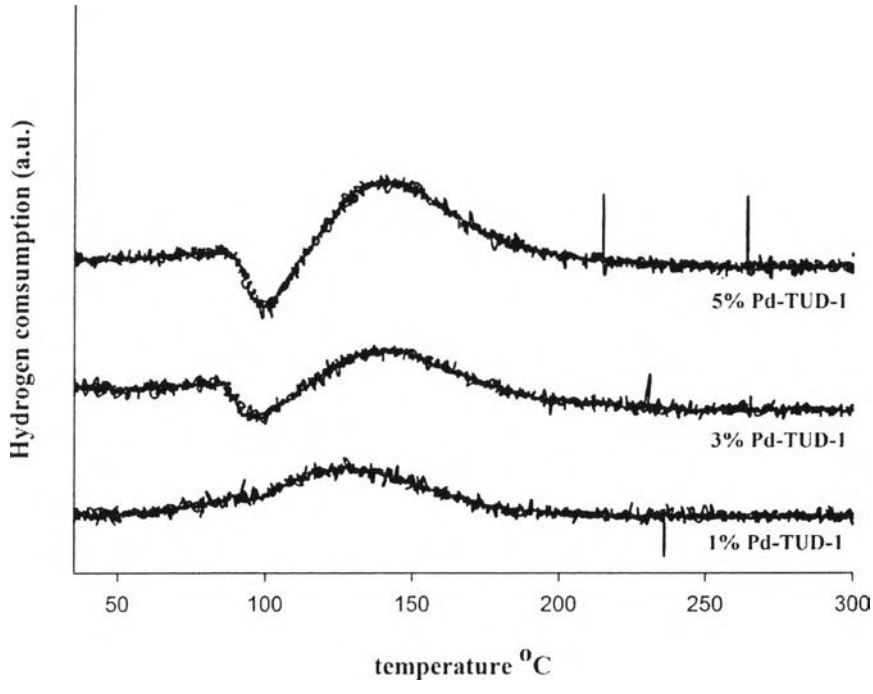

Figure 4.9 The TPR results of Pd-TUD-1 with various Pd amounts.

The broad peak at ca. 130°–140 °C observed in all samples attributed to the complete reduction of PdO, such a peak can be referred to the remnant of the PdO species which strongly interacted with the supports (Cubeiro *et al.*, 1998), as described by the equation below.

$$H_2 + PdO \longrightarrow Pd + H_2O$$

As increasing of the palladium loading, the more hydrogen participates in the reduction, resulting in the broader peak.

4.2 Catalytic activity

The catalytic activity of the synthesized Pd-TUD-1 catalysts was studied on Suzuki coupling reaction. The conversion yield of the products was determined by GC-MS analysis. This analytic method can also be used to identify the structure of the obtained products. Typically, the Suzuki coupling reaction originates from the mixture of arylboronic acid, aryl bromide, phosphine ligand containing Pd-catalyst, base, and organic solvent (McDaniel *et al.*, 2011). The phosphine ligand containing Pd-catalysts accelerate the oxidative addition and reductive elimination processes due to their strong σ-donor and weak π-acceptor properties. The bulky ligands make the catalyst be good acceptors of electron density from the Pd-metal center, such as $Pd(PPh_3)_4$ and $PdCl_2(PPh_3)_2$. Although phosphine ligands are conventionally used to activate the catalysts in the Suzuki coupling reaction and give excellent results, these ligands are generally air-sensitive. Thus, use of the phosphine ligand containing Pd-catalysts required air-free conditions, which are inconvenient and limit some synthetic applications (Hsu *et al.*, 2007).

On the other hand, Chang *et al.* (2012) developed another type of Pd-catalyst for the Suzuki coupling reaction by applying MCM-41 or SBA-15 silica materials to support $[Pd(NH_3)_4]Cl_2$, which is not air-sensitive and becomes more convenient than the use of phosphine-based Pd catalysts. Based on the size of the Suzuki coupling reaction product and the pore size on both MCM-41 and SBA-15, TUD-1 was thus used as the support for Pd in this study since the pore size of TUD-1 is larger than that of MCM-41 and SBA-15. Similar to MCM-41 or SBA-15, this Pd-TUD-1 catalyst is also air/moisture stable, opposite to pure Pd metal and other phosphine-based Pd catalysts. In this study, Pd-TUD-1 catalyst prepared via impregnation provided only PdO, as confirmed by XRD results. Therefore, when this PdO-related catalyst was used in the Suzuki reaction, the activity was expectedly less effective than those using $Pd(PPh_3)_4$ and $PdCl_2(PPh_3)_2$, containing mainly Pd^0. Scheme 4.1 shows the Suzuki coupling reaction in this work using phenylboronic acid to react with 1-bromo-4-fluorobenzene and Pd-TUD-1 catalyst in DMF solvent in the presence of K_2CO_3 base to produce the desired 4-fluorobiphenyl product and

by-product, namely, 1-bromo-3-fluorobenzene. According to Chang's study, our mechanism was proposed, as shown in Fig. 4.10.

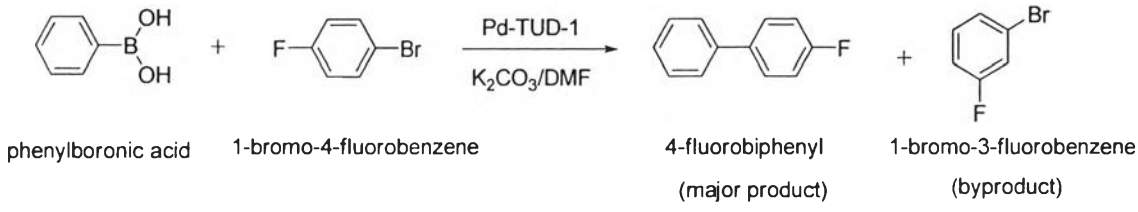

Scheme 4.1 The Suzuki coupling reaction in this work.

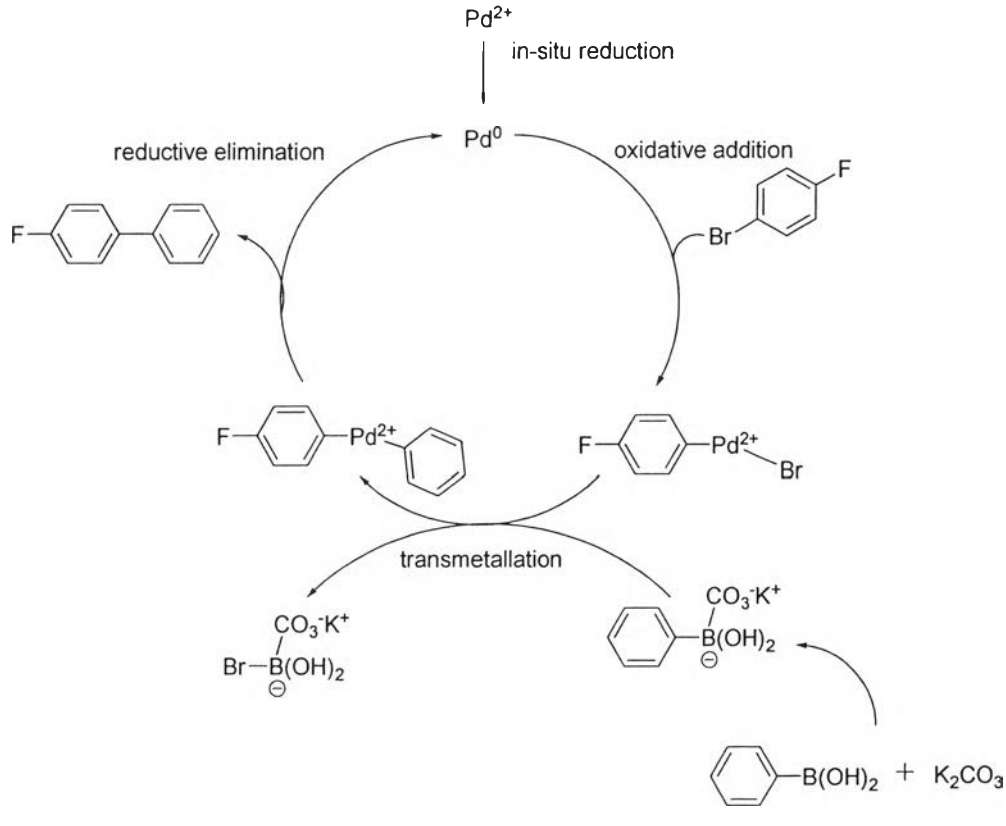

Figure 4.10 The proposed mechanism of this work.

The results of the Suzuki reaction using 1, 3, and 5% Pd-TUD-1 catalysts at various reaction durations of 10, 20, and 30 min are shown in Table 4.3. The results indicate that the reaction using 1% Pd-TUD-1 gave no desired product even at 30 min. This is not surprising since from the XRF results, 1% Pd-TUD-1 actually contained very small amount of Pd, thus resulting in very low or no activity. As

increasing Pd content to 3 and 5%, a small amount of the product started to occur. From Table 4.3 the shortest reaction time (10 min) provided the highest yield of the product conversion.

Table 4.3 GC-MS analysis of Pd-TUD-1 catalytic activity using K_2CO_3 base at 120 °C and 300 W microwave temperature and power, respectively

Catalyst	Time (min)	% Conversion	% Selectivity	
			major product	byproduct
TUD-1	10	-	-	-
	20	-	-	-
	30	-	-	-
1% Pd-TUD-1	10	-	-	-
	20	-	-	-
	30	-	-	-
3% Pd-TUD-1	10	17	100	-
	20	1	100	-
	30	2	50	50
5% Pd-TUD-1	10	20	100	-
	20	6	100	-
	30	14	29	71

The increase of the reaction time caused Pd-TUD-1 to have less stability under microwave irradiation, as described by Dawood *et al.* (2007). MEČIAROVÁ *et al.* (2001) also mentioned that the increase of reaction time in microwave-assisted reaction could cause several unidentified products mixed in the desired products of the corresponding reaction. This is probably why we obtained less desired product and more by-products as increasing the microwave reaction time. It is worth noting that for 5% Pd-TUD-1, percent conversion at 20 min reaction is less that that at 30

min reaction time. However, considering the percentage of the desired product, the 20 min reaction time was better since the 30 min reaction time resulted in higher by-product yield, i.e. 3-bromo-fluorobenzene. This by-product is probably caused by the direct reaction between the base (K_2CO_3) and the substrate (p-bromofluorobenzene) via benzyne intermediate (Djakovitch *et al.*, 1999), as illustrated in Fig. 4.11.

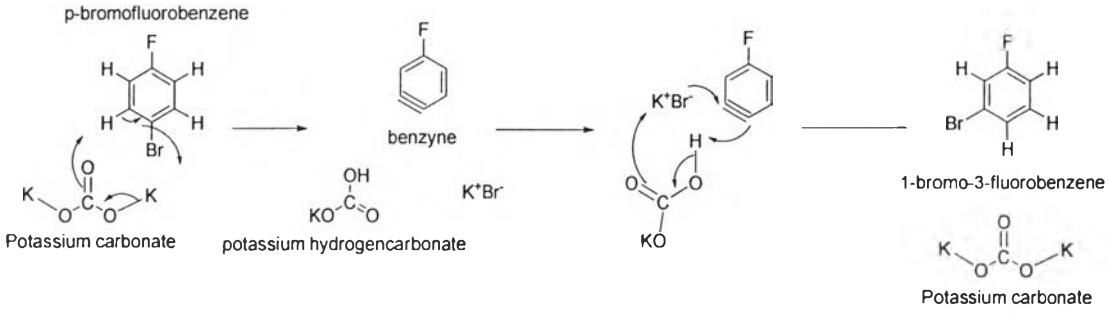

Figure 4.11 The proposed mechanism for by-product formation

This reaction is similar to the work described by Djakovitch in 1999. In conclusion, short reaction time gave the highest percent conversion and the amount of the product in Suzuki reaction indeed depends on the amount Pd concentration loaded on TUD-1. That is, the higher Pd content in Pd-TUD-1 provided the higher product yields.

Our results using Pd-TUD-1 catalysts provided less product yield than those using other types of Pd-catalyst done by McDaniel *et al.* (2011) and Chang *et al.* (2012). This can be explained as follows: The Pd species used in the Suzuki coupling reaction should be Pd° which is the important species in the oxidative addition step and this step is often the rate-determining step in the catalytic cycle. However, the Pd species in Pd-TUD-1 is PdO which is much more inert than Pd° (Phan *et al.*, 2006). Moreover, it is difficult to convert PdO into Pd^0, but it can be slightly reduced by organobron compound, i.e. phenylboronic acid (Masuyama *et al.*, 2012). Referring to the study by Chang *et al.* (2012), they introduced a heterogenous Pd catalyst, similar to our work, but they used $[Pd(NH_3)_4]Cl_2$ where the presence of tetra-amine ligand is capable of donating the electron of N to the Pd metal center and forming a complex (Chu *et al.*, 2010). Thus, this tetra-amine ligand acts a similar function to the

phosphine ligand in $Pd(PPh_3)_4$ and $PdCl_2(PPh_3)_2$. In addition, the use of water either as a solvent or a co-solvent can help the solvation of these substrates which are the organic-insoluble materials (Leadbeater *et al.*, 2005). However, in this work, we used only DMF as a solvent, causing incomplete solubility.

In summary, the best reaction time for Pd-TUD-1 catalyst in Suzuki coupling reaction was 10 min, in agreement with Chang *et al.* (2012), and, the more Pd content in Pd-TUD-1 resulted in the more products obtained from the Suzuki reaction.

As discussed previously, the Pd-TUD-1 catalysts used in our work is mostly in PdO form which was mentioned to be inappropriate for the Suzuki reaction. The species studied for this reaction was in the Pd^0 form. To test this assumption, we further carried out an additional experiment to convert the PdO species into the Pd^0 prior to the Suzuki reaction study. In this study, only 5%Pd-TUD-1 was chosen to be the case study. The conversion was achieved by flowing hydrogen gas along this catalyst in a batch reactor at a temperature of 300°C for 1 h. The color of the 5%Pd-TUD-1 catalyst was changed from red-brown to black, implying the complete conversion of PdO into Pd^0.

The Suzuki reaction activity of Pd^0 in 5%Pd-TUD-1 at 10 min reaction time indeed increased the %conversion from 20 to 32 while the %selectivity still maintained at 100. This might confirm that Pd^0 is an important active species for this type of reaction, as described in the previous section.